The Seventh Asia-Pacific Conference on Wind Engineering, November 8-12, 2009, Taipei, Taiwan

THE EFFECTS OF URBAN HEAT ISLAND MITIGATION STRATEGIES ON THE OUTDOOR THERMAL ENVIRONMENT IN CENTRAL TOKYO – A NUMERICAL SIMULATION –

Jou-Man Huang,[1] Ryozo Ooka,[2] Akiko Okada,[3] Toshiaki Omori,[4] and Hong Huang [5]
[1] *Graduate Student, Department of Architecture, University of Tokyo*
Tokyo 153-8505, Japan, jouman@iis.u-tokyo.ac.jp
[2] *Professor, Department of Architecture, University of Tokyo,*
Tokyo 153-8505, Japan, ooka@iis.u-tokyo.ac.jp
[3] *Fundamental Technology Department, Tokyo Gas Co., Ltd.,*
Tokyo 230-0045, Japan, a_okada_tg@yahoo.co.jp
[4] *Doctor, Fundamental Technology Department, Tokyo Gas Co., Ltd.,*
Tokyo 230-0045, Japan, omori@tokyo-gas.co.jp
[5] *Assistant Professor, Department of Architecture, University of Tokyo,*
Tokyo 153-8505, Japan, hhong@iis.u-tokyo.ac.jp

KEYWORDS: URBAN HEAT ISLAND, MITIGATION STRATEGY, OUTDOOR THERMAL ENVIRONMENT, NUMERICAL SIMULATION, SET*, EXPOSURE LIMITATION TIME

ABSTRACT

This research analyzed the effects of strategies to mitigate urban heat islands by means of numerical simulation, as applied to an actual street block in central Tokyo (Marunouchi district). The analysis method consisted of heat transfer calculations, CFD calculations, and evaluation of the effectiveness at mitigating an urban heat island. The results of this study demonstrated that covering roadways with water-permeable materials, and planting grass and trees on-site could reduce air temperatures and MRT, whereas covering roadways with highly reflective paint would increase MRT and SET*, and lead to environmental degradation.

Introduction

As the urban heat island phenomenon has become dramatically worse over the last few decades, there have been quite a number of studies concerning strategies to mitigate such urban heat islands. However, these studies have mostly focused on analysis of the strategies with simple street blocks, while a few studies are based on actual street blocks. Furthermore, in most of the past studies based on actual street blocks, any greenery considered has usually only been grass, not trees, and approached the simulation results by simply changing the evaporation rate of the surface material. As a result, the greenery simulations could not realistically reflect the actual conditions of real street blocks. Therefore, this research has incorporated a tree model (Yoshida et al., 2000) to explore the difference in results between "planting" and "not planting" trees.

On the other hand, past research discussing mitigation strategies for urban heat islands have usually evaluated the thermal environment using the Standard New Effective Temperature (SET*) index produced by ASHRAE. Also the developed index was experimented on in a specific range for the purpose of human body comfort environment, so it may not be appropriate for very hot summers, such as when the temperature reaches 35°C. In addition, where the examinees were European or American, there may also be some

physiological deviation from Asians. For the above reason, this research would use SET*(Gagge et al., 1986) as revised (by Minami et al., 2006; Ooka et al., 2008) and the exposure limitation time that resulted from water-loss due to sweating to evaluate the thermal environment.

The purpose in this paper is to apply a numerical simulation to an actual street block in central Tokyo (Marunouchi district) and to analyze the effects of mitigation strategies for urban heat islands (Chen et al., 2004). The main strategies analyzed are listed as follows: (1) planting grass or painting highly reflective coatings on rooftops, (2) covering roadways or the site with water-permeable materials or highly reflective paint and planting grass, and (3) planting trees onsite.

Summary of analysis process

Analysis process

This research was mainly divided into two analytical steps. The first was to simulate the outdoor actual conditions in the Otemachi, Marunouchi, and Yurakucho districts of Tokyo. The second step was to simulate the outdoor thermal environment according to the proposed mitigation strategies.

Analysis subjects

The research area is shown in Figure 1, and the modeling meshes were generated to simulate the actual outdoor conditions in the Otemachi, Marunouchi, and Yurakucho districts of Tokyo. However, the proposals for mitigation strategies regarding the outdoor thermal environment are limited to the area highlighted within the dashed line (Marunouchi district).

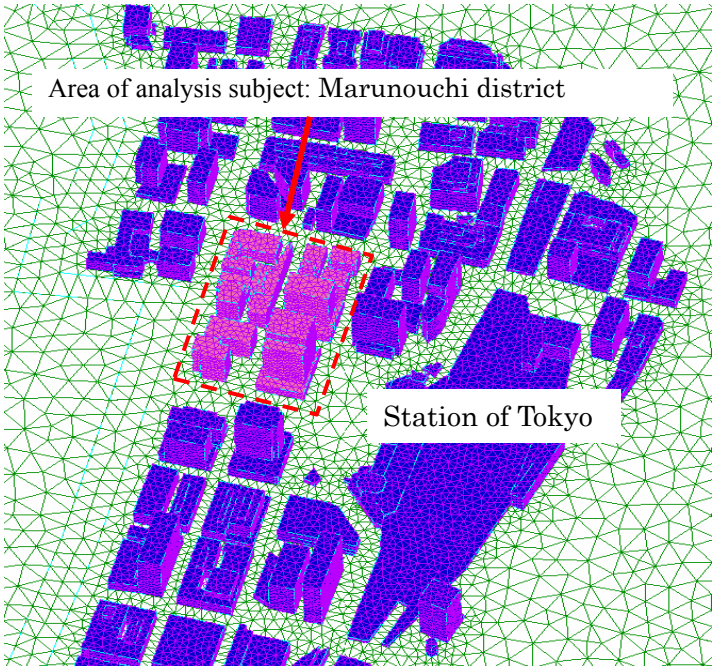

Figure 1: Research area of study

Analysis cases

Eight cases are analyzed in this paper as shown in Table 1. Case 1 was a control case and represents the standard condition without any improvement strategy for urban heat islands (the actual outdoor conditions in the Otemachi, Marunouchi, and Yurakucho districts of Tokyo). Cases 2 and 3 were conducted under conditions where the rooftop was covered in

greenery and highly reflective paint respectively; Cases 4 to 7 were conducted under various roadway or site conditions, and Case 8 was conducted assuming trees were planted onsite.

Table 1. Parameter settings for analysis cases

Case		Road		Site			Rooftop		
		α	β	α	β	trees	α	ε	β
1	Control case	0.9	0	0.9	0	none	0.8	0.9	0
2	Rooftop: greenery	0.9	0	0.9	0	none	0.8	0.95	0.3
3	Rooftop: highly reflective paint	0.9	0	0.9	0	none	0.5	0.9	0
4	Roadway: water-permeable cover Site: greenery	0.9	0.3	0.8	0.3	none	0.8	0	0
5	Site: greenery	0.9	0	0.8	0.3	none	0.8	0	0
6	Rooftop: highly reflective paint	0.5	0	0.9	0	none	0.8	0	0
7	Roadway: highly reflective paint Site: greenery	0.5	0	0.8	0.3	none	0.8	0	0
8	Site: planting tree	0.9	0	0.9	0	planted	0.8	0.9	0

α: shortwave radiation rate β: evaporation rate ε: longwave radiation rate

Analysis method and parameter settings

The analysis method in this paper consisted of three main parts. The first part was a heat transfer calculation, and used a three-phase calculation composed of shortwave calculation, convection-radiation transfer calculation, and unstable heat-conduction calculation, to estimate the surface temperature of buildings or land. The second part, a fluid calculation, used the surface temperature at a certain point in time that results in a heat transfer calculation as an initial value to estimate the distribution of air temperature, wind, and humidity in outdoor space. The third part used a revised SET*, mean radiant temperature (MRT), and exposure limitation time as indices of thermal environments to evaluate the effectiveness at reducing urban heat islands.

Heat transfer calculation

The analysis period for the heat transfer calculation was the 48 hours from July 22 at 12:00 a.m. to July 23 at 12:00 p.m. The air temperature data for each hour referenced the Meteorological Agency's database. For the other base settings, the convection transfer rate was set as 11.6 W/m^2K outdoor and 4.64 W/m^2K indoor; the temperature setting was a constant 26°C indoors and in soil at 0.5-m depth, the evaporation rate for water-permeable materials covering the roadway, planted grass, and greenery on the rooftop was a constant 0.3; and the physical properties of the surface materials are presented in Table 2.

Table 2. Physical properties of surface materials

Place	*Material*	*Reflection rate of shortwave radiation*	*Emission rate of longwave radiation*	*Heat transmission rate*	*Specific heat of capacity*	*Thickness*
		-	-	*W/mK*	*kJ/m^3K*	*m*
Buildings	concrete	0.2	0.9	1.64	1900	0.2
Ground	asphalt	0.2	0.95	0.73	2100	0.1
Underground	gravel			0.62	1500	0.1
	soil			1.5	3100	0.3

Computational fluid dynamics (CFD) calculation

The analysis period for the CFD calculation was 3:00 p.m. on July 23. In terms of the income boundary conditions, the surface temperature resulting from the heat transfer calculation was designed as the temperature, the wind vector was southerly at 3 m/s, air temperature was 31.5°C, and the water vapor pressure was 2.8 kPa. The setting details for the CFD calculation are shown in Table 3.

Table 3. Setting details for CFD calculation

Turbulence model	High Reynolds number k-ε model		
Calculation algorithm	SIMPLE		
Differential Skill	Advection item: Differential liner windward equation		
Convective heat transfer coefficient	α_c: 11.6 [W/m^{2}K]		
Boundary conditions for calculation area	Sky, east side, west side	slip	Temperature of sky
	South side	Flow-out	Temperature of sky
	North side	Flow-in	Temperature of sky
Boundary conditions for flow-in side	Wind speed: $U(z)=Us(z/z_s)^{\alpha}$ α=0.35, z_s=74.5 U(z): wind speed at height of z m [m/s] Us: wind speed at standard height of z_s m [m/s]		
	Turbulent energy: $K(z)=(I(z)U(z))^2$ [m^2/s^2] $I(z)=0.1(z/z_G)^{(-\alpha-0.05)}$, z_G=650 m		
	The dissipation coefficient of k: $\varepsilon(z)=C_\mu 1/2\ k(z)\ (u_s/z_s)\ \alpha\ (z/z_s)^{(\alpha-1)}$ [m^2/s^3] C_μ=0.09		
Latent heat of evaporation	$L_w = \alpha_W \beta\ L(f_{aP} - f_{sP})$ α_w: transfer coefficient of water vapor [kg/m^{2}skPa] ($=7.0\times10^{-6}\alpha_c$) β: efficacy of evaporation [-] L: latent heat of evaporation ($=2.5\times10^6$ [J/kg]) f_{aP}: water vapor around tree [kPa] f_{sP}: saturated water vapor of land surface [kPa]		

SET, MRT, and exposure limitation time*

The parameter settings for the SET*, MRT, and exposure limitation time are shown in Table 4. The MRT calculation was established with a factor of 0.5 for the shortwave absorption rate by human body, and 0.95 for longwave. The sweating model used in SET* calculation was modified by the authors (Minami et al., 2006). In terms of the settings for the human condition, the height was 162 cm, weight 59 kg, surface area was 1.62 m^2, the clothing insulation value was 0.5 clo, and the function of activity level was 2 Met. In terms of the exposure limitation time, it was set as the time at which water loss due to sweating totaled 3% of body weight, or the core human temperature reached 38°C.

Table 4. Parameter settings for SET*, MRT, and exposure limitation time

MRT		***Human thermal physiological model***		***Exposure limitation time***	
Absorption rate of shortwave radiation	0.5	Height	161.9 cm	Loss of water	3% weight
Absorption rate of longwave radiation	0.95	Weight	59.0 Kg	Core human temperature	38°C
		Body surface area (based on DuBois formula)	1.62 m^2		
		Clothing levels	0.5 clo		
		Metabolic equivalent	2 Met		

Tree model

The arrangement of the tree model in this research is shown in Fig. 2. The parameter settings for trees are as shown in Table 5. The tree height was 7 m, the height of the bottom of the tree canopy was 2.5 m, the width of the tree canopy was 3 m, trees were planted 9 m apart, with 102 trees in total. In addition to other settings with regard to the tree model, the extinction coefficient was a constant 0.6, leaf area density was a constant 0.4 m^2/m^3, while the emissivity of shortwave radiation was 0.85 and of longwave radiation was 0.98.

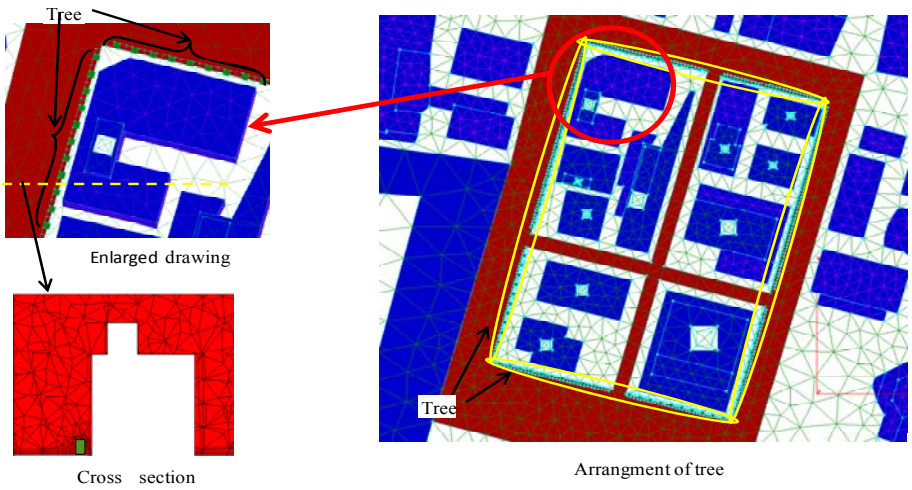

Figure 2: Arrangement of the tree model in this research

Table 5. Tree parameter settings

Basic condition of tree		***Parameter settings of tree***	
Tree height	7 m	Extinction coefficient	0.6
Height of underside of tree canopy	2.5 m	Leaf area density	0.4 m^2/m^3
Tree canopy width	3 m	Emissivity of shortwave radiation	0.85
Interval between trees	9 m	Emissivity of longwave radiation	0.98
Total number of trees	102		

Analyzed results for an actual street block in central Tokyo

Heat received from shortwave radiation at surface

By calculating the direct shortwave radiation and shortwave radiation reflected from the sky and surfaces, the results of the heat received are shown in Fig. 3. These results demonstrated that heat received from shortwave radiation from road surfaces near buildings was highest.

Temporal change and distribution of surface temperature

The temporal changes in surface temperature are shown in Fig. 4. Figure 5 shows the distributions of surface temperature at 9:00, 12:00, and 15:00 hours. The surface temperature at the rooftop was relatively high because of the direct shortwave radiation received. In the area with most greenery (Imperial Palace area), the surface temperature was relatively lower due to evaporation via plants. In terms of buildings and the ground, the surface temperatures were markedly different between areas of sunshine and shade.

Distribution of air temperature and wind speed

The distribution of air temperature at 1.5-m height is shown in Fig. 5. Figures 6 & 7 map the wind vectors and speeds. From these figures, it is clear that areas with relatively high surface temperatures also tend to have higher air temperatures. However, wind speeds were different from place to place. In particular, wind speeds were very low in the spaces between buildings.

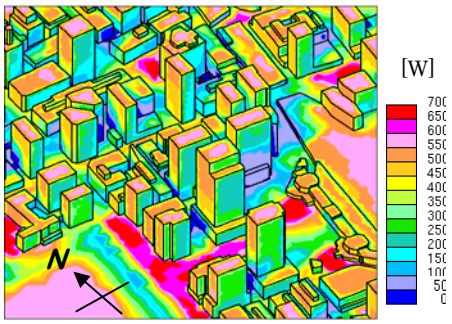

Figure 3 : Heat received from shortwave radiation at surface

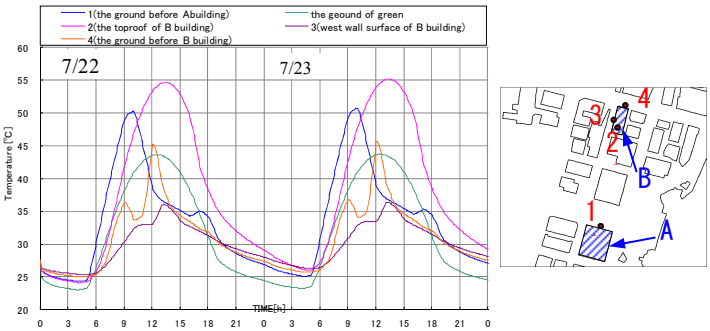

Figure 4 : Temporal change of surface temperature

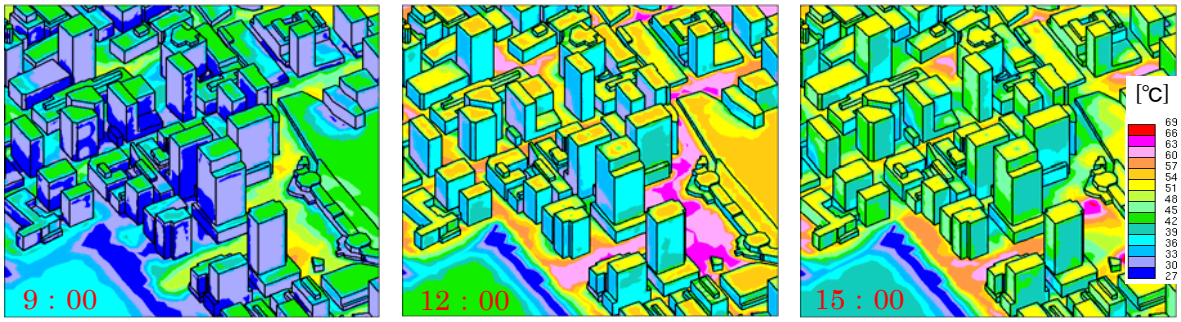

Figure 5 : Distribution of surface temperature

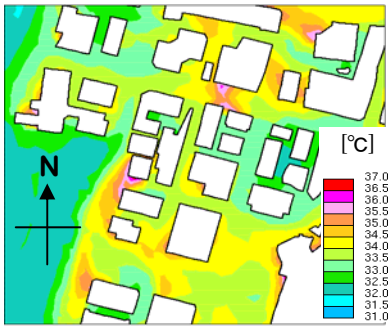

Figure 6: Distribution of air temperature

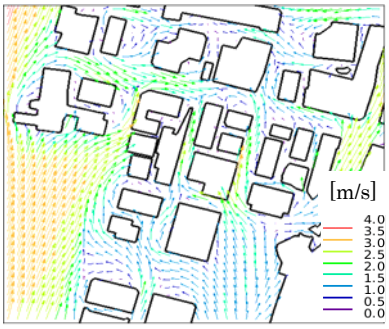

Figure 7: Vector of wind speed

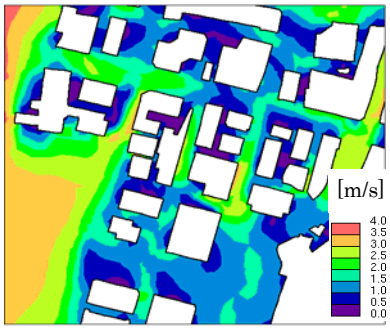

Figure 8: Wind speed

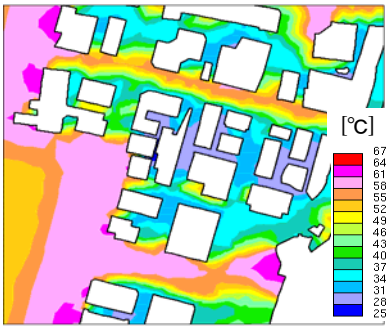

Figure 9 : Distribution of MRT

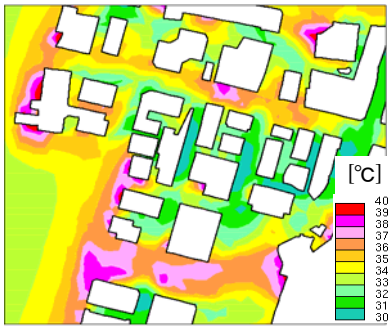

Figure 10: Distribution of SET*

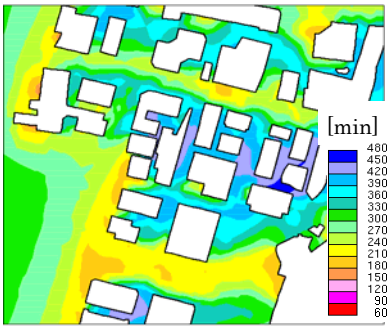

Figure11: Distribution of exposure limitation time

Evaluation of outdoor thermal environment

The distribution of air temperature at 1.5-m height is shown in Fig. 9, which demonstrated that values are higher at roads near buildings, and lower in shaded areas. The distribution of SET* is shown in Fig. 10, which also demonstrates the values around the buildings that received direct shortwave radiation are larger. The distribution of exposure limitation time is shown in Fig. 11, which demonstrated the time values at places with large SET* are usually shorter.

Analyzed result of strategic improvement proposals

Distribution of surface temperature

The distribution of surface temperature in Case 1 is shown in Fig. 12(a). Greenery on the rooftop reduced the surface temperature of the wall near the top of the building by 1°C (Fig. 12(b)). Covering roadways with water-permeable materials and planting grass on the site cut the surface temperature of the road by 18°C, and the surface temperature of the wall was reduced by 1°C (Fig. 12(c)). Covering the roadway with highly reflective paint reduced the surface temperature of the road by 13°C, but increased the surface temperature of the nearby wall by 1°C (Fig. 12(d)). Planting trees on the site resulted in a reduction in the surface temperature of the site under the tree canopy by up to 11°C (Fig. 12(e)).

Distribution of air temperature

The distribution of air temperature at 1.5-m height is shown in Fig. 13. Greenery on the rooftop had no effect on the air temperature in pedestrian areas (Fig. 13(b)). Covering roadways with water-permeable materials and planting grass on the site can decease the temperature by about 1°C in pedestrian areas (Fig. 13(c)). Covering the roadway with highly reflective paint had some effect in deceasing the air temperature in pedestrian areas (Fig. 13(d)). There was no noticeable thermal effect in pedestrian areas by planting trees on the site (Fig. 13(e)).

Distribution of MRT

The distribution of MRT at 1.5-m height in Case 1 is shown in Fig. 14(a). Greenery on the rooftop did not affect the MRT in pedestrian areas (Fig. 14(b)). The effect of covering roadways with water-permeable materials and planting grass on the site mostly reduced the MRT by about 1°C at 1.5 m higher (Fig. 14(c)). The effect of covering the roadway with highly reflective paint increased the MRT by about 2°C (Fig. 14(d)). The effect of planting trees on the site cut the MRT by up to about 10°C at 1.5-m height (Fig. 14(e)).

*Distribution of SET**

The distribution of SET* at 1.5-m height is shown in Fig. 15. Covering roadways with water-permeable materials and greenery on the site decreased the SET* by about 1°C in pedestrian areas (Fig. 15(c)). However, covering the roadway with highly reflective paint increased the SET* by about 0.3°C (Fig. 15(d)). Planting trees on the site decreased SET* by about 2°C at most in pedestrian areas under the tree canopy (Fig. 15(e)).

Distribution of the exposure limitation time

The distribution of exposure limitation time is shown in Fig. 16. In Case 1, the exposure limitation time was about 3 hours. Covering the roadway with water-permeable materials and greenery on the site can extend that by about 80 minutes at most (Fig. 16(c)). However, covering the roadway with highly reflective paint reduced the exposure limitation time by 20 minutes (Fig. 16(d)). Planting trees on the site could extend the exposure limitation time by up to 65 minutes at most in pedestrian areas under the tree canopy (Fig. 16(e)).

Conclusions

According to the results from analyzing an actual street block in central Tokyo, the principal findings are:

1. The surface temperature experienced significant difference with temporal change, and there was also a great difference between sunny and shaded areas on the ground or buildings.
2. The heat received from shortwave radiation on the surface was strongly related to air temperature, MRT, SET*, and exposure limitation time.

According to the analyzed results of mitigation strategies regarding urban heat islands, the principal findings are:

1. Covering roadways with water-permeable materials, and planting grass and trees on the site could reduce the surface temperature and MRT, and extend the exposure limitation time, which had a marked easing on the thermal environment as well.
2. Covering roadways with water-permeable materials and planting grass on the site also could reduce the air temperature in pedestrian areas to ease the outdoor thermal environment. However, the effect of planting trees on the site was somewhat limited. The reason may be that the total amount or mass volume of planted trees was too small – relative to the total street block space – to reduce the air temperature in pedestrian areas.
3. Although covering roadways in highly reflective paint could reduce the air temperature, it also caused an increase in the MRT and SET*, leading to environmental degradation.

References

Chen H., Ooka R., Harayama K., Kato S., Li X. (2004), "Study on Outdoor Thermal Environment of Apartment block in Shenzhen, China with coupled simulation of convection, radiation and conduction", Energy and Building, 36, 1247~1258.

Gagge A.P., Fobelets A.P., Berglund P.E. (1986), "A Standard Predictive Index of Human Response to The Thermal Environment", ASHRAE Transactions, 92(1), 709~731.

Minami Y., Ooka R., Tsuzuki K., Sakoi T., Sawasaki S. (2006), "Study on Human Physiological Models for Hot Environments", Sixth International Thermal Manikin and Modeling Meeting Preprints, Hong Kong, China, October 16~18, 89~97.

Ooka R., Yuriko M., Tomonori S., Kazuyo T. (2008), "Study on human physiological models for hot environments", 11th International Conference on Indoor Air Quality and Climate, Copenhagen, Denmark, August 17~22.

Yoshida S., Ooka R., Mochida T. (2000), "Study on Effect of Greening on Outdoor Thermal Environment Using Three Dimensional Plant Canopy Model", Journal of Architecture, Transactions of AIJ, 536, 87~94.

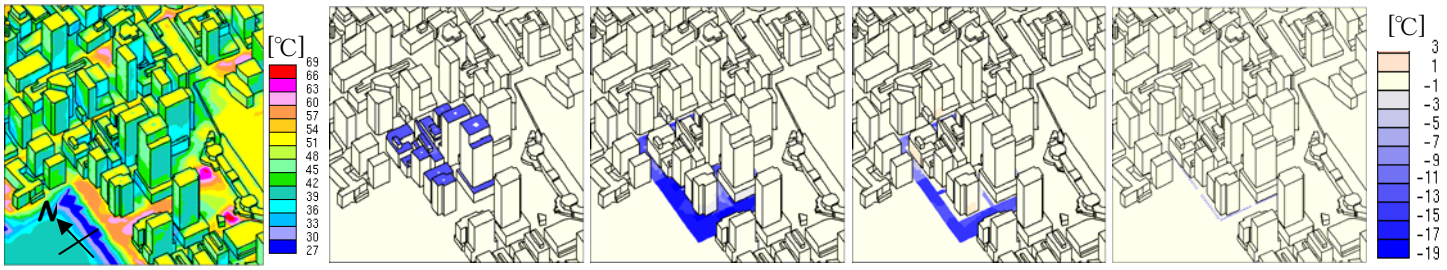

(a) case1 (b) case2-case1 (c)case4-case1 (d)case6-case1 (e)case8-case1

Figure 12: Distribution of surface temperature（15:00）

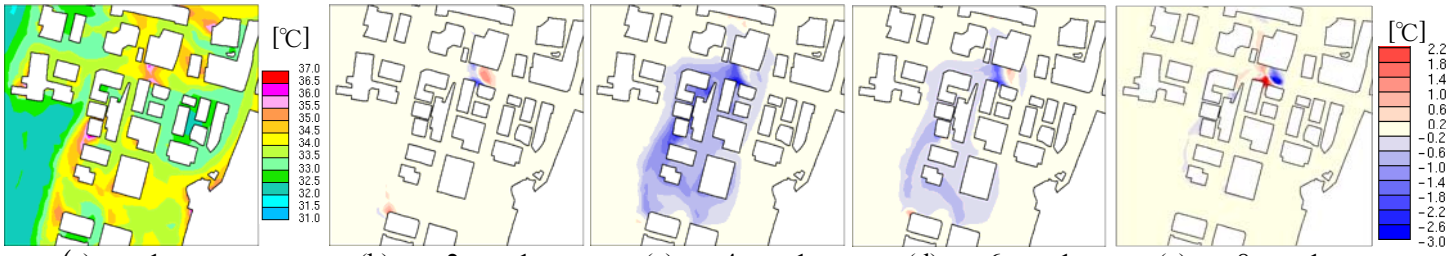

(a) case1 (b) case2-case1 (c)case4-case1 (d)case6-case1 (e)case8-case1

Figure 13: Distribution of air temperature（15:00）

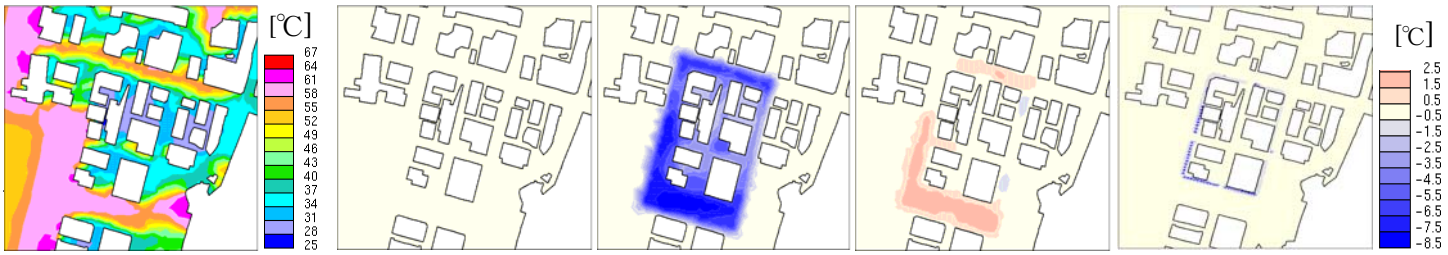

(a) case1 (b) case2-case1 (c)case4-case1 (d)case6-case1 (e)case8-case1

Figure 14: Distribution of MRT（15:00）

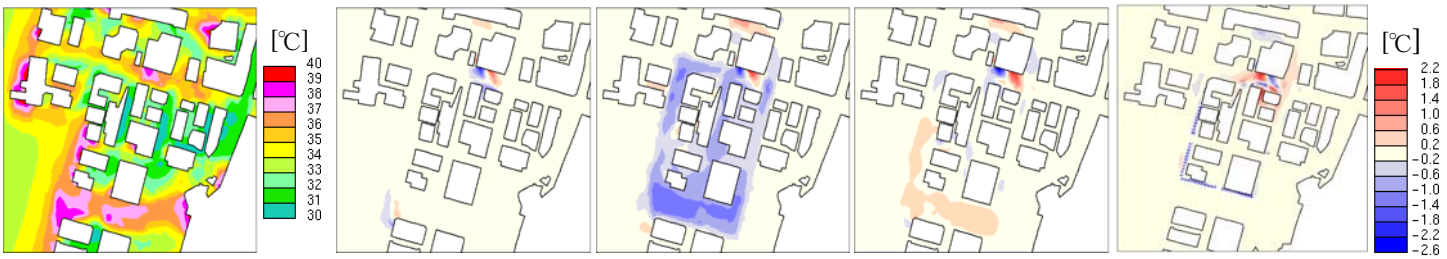

(a) case1 (b) case2-case1 (c)case4-case1 (d)case6-case1 (e)case8-case1

Figure 15: Distribution of SET*（15:00）

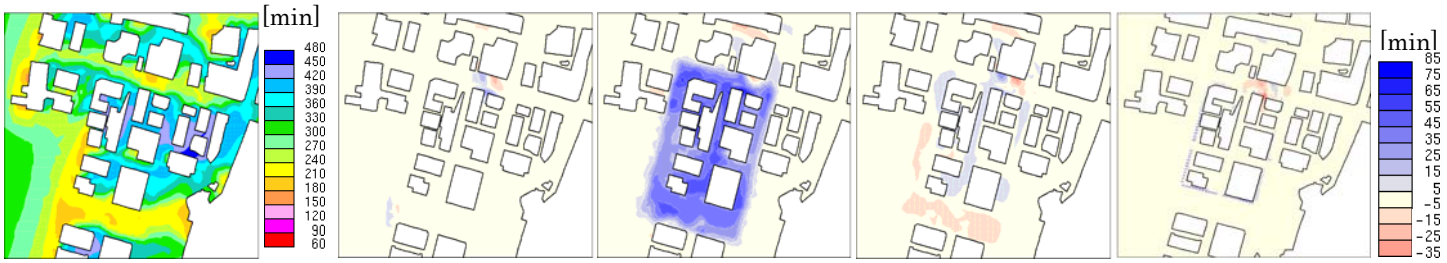

(a) case1 (b) case2-case1 (c)case4-case1 (d)case6-case1 (e)case8-case1

Figure 16: Distribution of the exposure limitation time（15:00）